An improved-SFIM fusion method based on the calibration process ☆

Zhenyu An[a], Zhenwei Shi[a,*]

[a]*Image Processing Center, School of Astronautics, Beihang University, Beijing 100191, P.R. China*

Abstract

The fusion of multispectral/hyperspectral image (MSI/HSI) and panchromatic image (PI) is a crucial and useful issue. Among the different fusion methods, smoothing-filter-based intensity modulation (SFIM) fusion technique is a simple yet effective model. It is proposed based on a simplified solar radiation and land surface reflection model. However, the calibration process, which is important in the remote sensing, is neglected. Meanwhile, in the fusion model, instead of using the accurate radiance value, the digital number (DN) value of optical image is improperly used. It caused the distortion of color in the fused images. Therefore, in the letter, we propose an improved-SFIM (ISFIM) by exploiting the calibration process. In the model, the range of DN values of the fused data are properly constrained in the calibration process. Experiments on the MSI and HSI are presented along with the fusion results obtained by discrete wavelet transform, Gram-Schmidt transform, original SFIM techniques and the proposed ISFIM. The results illustrate that, the ISFIM behaves better both in visual analysis and objective indices than existing methods.

Keywords: Smoothing-filter-based Intensity Modulation (SFIM),

☆The work was supported by the National Natural Science Foundation of China under the Grants 61273245 and 91120301, the 973 Program under the Grant 2010CB327904, the open funding project of State Key Laboratory of Virtual Reality Technology and Systems, Beihang University (Grant No. BUAA-VR-12KF-07), and Program for New Century Excellent Talents in University of Ministry of Education of China under the Grant NCET-11-0775. The work was also supported by Beijing Key Laboratory of Digital Media, Beihang University, Beijing 100191, P.R. China.

*Corresponding author. Tel.: +86-10-823-39-520; Fax: +86-10-823-38-798.

Email address: shizhenwei@buaa.edu.cn (Zhenwei Shi)

Calibration Process, Multispectral/Hyperspectral Image Fusion, Quality Assessment.

1. Introduction

Image fusion for multispectral/hyperspectral images (MSI/HSI) has being attracting more and more people's attentions. Different fusion methods have been proposed for the useful yet still challenging work.

The various existing fusion methods could be sorted into several basic categories: arithmetic methods, projection-substitution-based methods, ARSIS (the French acronym for "Amélioration de la Résolution Spatiale par Injection de Structures", which represents Improving Spatial Resolution by Structure Injection) concept fusion methods, model-based methods, and hybrid methods. The arithmetic methods cost less computational time relatively, but the fused data usually has serious spectral distortion [1]. Projection-substitution-based methods, like intensity hue saturation (IHS) [2] and Gram-Schmidt (GS) [3] transform, are all typical widely used methods. For methods based on the ARSIS, the high-frequency information is extracted from the panchromatic images (PIs) and then injected into the MSIs/HSIs. Discrete wavelet transform (DWT) [4], "á trous" wavelet transform (ATWT) [5, 6], additive-wavelet luminance proportional method (AWLP) [7], and so forth, have been used to accomplish the task of fusion. Model-based methods are usually based on image formulation models and some strong theoretical frameworks. Projection onto convex sets (POCS) [8] and variational fusion methods [9] are the representative methods. Hybrid methods such as the Ehlers method [10] (combination of the IHS method and the ARSIS method) synthesize the virtues of different fusion methods.

As one of the effective methods, smoothing-filter-based intensity modulation (SFIM) [11] is proposed by J. G. Liu. It is an useful fusion method based on a simplified solar radiation and land surface reflection model. In a reply [14] to a critical comment [15] on this method, Liu deeply discussed its principles and rationalities. The method minimizes the spectral distortions while improving the spatial quality of the MSI/HSI. The original SFIM model is derived from relations between the digital number (DN) value in image, the solar radiation impinging on the land surface, irradiance $E(\lambda)$, and the spectral reflectance of the land surface $\rho(\lambda)$:

$$DN(\lambda) = \rho(\lambda)E(\lambda) \tag{1}$$

Its idea consists of two basic steps:

1. Obtain the degraded version of PI by using low-pass filtering, and then compute the ratio between the PI and the degraded version.

2. Obtain the fused image without changing its spectral information by the next calculating equation:

$$DN(\lambda)_{fus} = \frac{DN(\lambda)_{low} DN(\gamma)_{high}}{DN(\gamma)_{mean}} \tag{2}$$

where $DN(\lambda)_{fus}$, $DN(\lambda)_{low}$, $DN(\gamma)_{high}$, $DN(\gamma)_{mean}$ are the pixel values in the fused high-spatial-resolution MSI/HSI, original low-spatial-resolution MSI/HSI, original high-spatial-resolution PI, low-spatial-resolution PI (obtained by applying the low-pass filtering in the original PI), respectively.

However, Liu's SFIM model neglects the calibration process [12], which should be taken into consideration in equation (1). This leads to the distortion of the color in the fused MSI/HSI. Therefore, in the letter, we cogitate the fusion method again and propose an improved-SFIM (ISFIM) method. In Section 2.1, the original SFIM and calibration process is discussed in brief. In Section 2.2, we propose the new fusion method ISFIM. In the method, we establish more in-depth relationship between the DN of fused image and the original MSI/HSI. In Section 3, a comparison between different fusion techniques is presented. Results on both MSI and HSI are presented using both visual and quantitative evaluations. Finally, the letter closes with conclusions in Section 4.

2. ISFIM based on exploiting the calibration process

2.1. SFIM and the Calibration process

2.1.1. SFIM

SFIM is derived from the physical principle presented in equation (1). From this equation, we have:

$$DN(\lambda)_{low} = \rho(\lambda)_{low} E(\lambda)_{low} \tag{3}$$

$$DN(\gamma)_{high} = \rho(\gamma)_{high} E(\gamma)_{high} \tag{4}$$

where $DN(\lambda)_{low}$ represents a DN value in a lower resolution image of spectral band of spectral band λ, and $DN(\gamma)_{high}$ is the value of the corresponding pixel in a higher resolution image of spectral band γ. With the assumptions $E(\lambda) \approx E(\gamma)$ and $\rho(\gamma)_{high} \approx \rho(\gamma)_{low}$, the original equation (2) could be obtained from equation (1), and it is the original SFIM model.

2.1.2. Calibration process

Calibration process, which consists of absolute and relative calibration, is crucial in obtaining the remote sensing images. Usually, by a simple equation (5), the calibration process establishes the relationship among the radiance value (RV), the spectrometer obtained, and the DN value of the optical image.

$$RV_i = aDN_i + b \tag{5}$$

where DN_i and RV_i stand for the DN value and the RV of each pixel i in the optical image we obtained, respectively. Parameter a and b represent the gain value and offset value which obtained via a large number of experiments. Their values are usually not zeros.

The DN values of optical images, like PI, MSI, and HSI should be calibrated before they could be used. So the calibration process is an important step. However, it has been neglected in fusion model before, which leads to two problems. Firstly, it has to be clear that, DN is not equal to RV. So, the $DN(\lambda)$ in the left part of the equation (1) is not the actual value. It is not equivalent to the right of the equation. Actually, we believe that, the RV that the spectrometer received should be in the left of equation (1). On the other hand, the RV has more proper units with $\mathbf{W} \cdot \mathrm{cm}^{-2} \cdot \mathrm{sr}^{-1} \cdot \mathrm{nm}^{-1}$ than DN. Secondly, in the real system, the DN values of the images are within a certain range due to the bandwidth. This is also usually neglected in fusion process. Therefore, in the following discussion, we improve the SFIM by considering the mentioned problems.

2.2. Proposed ISFIM

As we have discussed in section 2.1.2, the equation (1) should be revised, and the DN should be replaced by RV. Therefore, we have:

$$RV(\lambda) = \rho(\lambda)E(\lambda) \tag{6}$$

Also, all the DN in the equation (2) should be replaced by RV, and the equation is obtained as follows:

$$RV(\lambda)_{fus} = \frac{RV(\lambda)_{low} RV(\gamma)_{high}}{RV(\gamma)_{mean}} \tag{7}$$

where $RV(\lambda)_{fus}$, $RV(\lambda)_{low}$, $RV(\gamma)_{high}$, and $RV(\gamma)_{mean}$ represent the radiance the spectrometer obtained in the fused image, the low-spatial-resolution

image, the high-spatial-resolution image, and the degraded version of high-spatial-resolution image, respectively. Notice that, all the RVs here are not the DN values of image we usually used. However, according to the calibration equation (5), we could establish their relations as follows:

$$RV(\lambda)_{fus} = a_{fus} DN(\lambda)_{fus} + b_{fus} \tag{8}$$
$$RV(\lambda)_{low} = a_{low} DN(\lambda)_{low} + b_{low} \tag{9}$$
$$RV(\gamma)_{high} = a_{high} DN(\gamma)_{high} + b_{high} \tag{10}$$
$$RV(\gamma)_{mean} = a_{mean} DN(\gamma)_{mean} + b_{mean} \tag{11}$$

where a_{fus}, a_{low}, a_{high}, a_{mean}, b_{fus}, b_{low}, b_{high} and b_{mean} are the gain and offset of those images mentioned in equation (7), respectively. Also, since the MSI/HSI and mean image are degraded from the fused MSI/HSI and the PI, respectively, we have the following approximations:

$$a_{fus} \approx a_{low} \tag{12}$$
$$b_{fus} \approx b_{low} \tag{13}$$
$$a_{high} \approx a_{mean} \tag{14}$$
$$b_{high} \approx b_{mean} \tag{15}$$

Substituting the RV of equation (7) with the above terms, then we have:

$$a_{low} DN(\lambda)_{fus} + b_{low} = \frac{(a_{low} DN(\lambda)_{low} + b_{low})(a_{high} DN(\lambda)_{high} + b_{high})}{a_{high} DN(\gamma)_{mean} + b_{high}} \tag{16}$$

The fused DN value could be obtained:

$$DN(\lambda)_{fus} \approx \frac{(a_{low} DN(\lambda)_{low} + b_{low})(a_{high} DN(\gamma)_{high} + b_{high})}{a_{low}(a_{high} DN(\gamma)_{mean} + b_{high})} - \frac{b_{low}}{a_{low}} \tag{17}$$

After simplification, we have the following fused result:

$$DN(\lambda)_{fus} = DN(\lambda)_{low}(k_1 \frac{DN(\gamma)_{high}}{DN(\gamma)_{mean}} + k_2) \tag{18}$$

where

$$k_1 = \frac{1 + \frac{b_{low}}{a_{low} DN(\lambda)_{low}}}{1 + \frac{b_{high}}{a_{high} DN(\gamma)_{mean}}} \tag{19}$$

$$k_2 = \frac{\frac{b_{high}}{a_{high} DN(\gamma)_{mean}} - \frac{b_{low}}{a_{low} DN(\lambda)_{low}}}{1 + \frac{b_{high}}{a_{high} DN(\gamma)_{mean}}} \tag{20}$$

According to the section 2.1.2, the range of DN value of the fused data should be limited. In the letter, we assume the fused date being close to the original MSI/HSI. That is to say, the range of term $k_1 \frac{DN(\lambda)_{high}}{DN(\gamma)_{mean}} + k_2 - 1$ could be limited by the following equation:

$$Ratio\_DN = \begin{cases} Ratio\_DN, & \text{if } -\delta \leq Ratio\_DN \leq \delta \\ \delta, & \text{if } Ratio\_DN > \delta \\ -\delta. & \text{else} \end{cases}$$

where $Ratio\_DN = k_1 \frac{DN(\lambda)_{high}}{DN(\gamma)_{mean}} + k_2 - 1$, and δ is a constant. Therefore, the ISFIM is obtained by the equation:

$$DN(\lambda)_{fus} = DN(\lambda)_{low}(Ratio\_DN + 1) \tag{21}$$

Thus, we have the ISFIM model. It is clear that, the fused data is affected by the calibrated parameters a and b. If we have these calibrated parameters before fusion, then the precise fusion results could be easily calculated. On the other hand, if the value of ratio $\frac{b}{a}$ equals zero, which means that the offset b equals zero, then $k_1 = 1$, $k_2 = 0$ are obtained. In this circumstance, the ISFIM degrades to the original SFIM as in equation (2). However, b is different because of different kinds of data. Moreover, b is even different for different bands of the same data though they have small difference. Here, we relax our calculation of k_1 and k_2, and use approximate value for the model. For the optical images like MSI/HSI and PI, their ratios are assumed similar to each other. Actually, the $\frac{b}{a}$ is usually less than 10. At the same time, the values of the same pixels in $DN(\lambda)_{low}$ and $DN(\gamma)_{mean}$ are similar and usually much larger than 10 in optical remote imagery, so $k_1 \approx 1$ is usually obtained in real data. This explains why SFIM is not available in fusion of optical image and synthetic aperture radar (SAR) image, for the parameters between optical and SAR images have great difference. On the other hand,

as we have mentioned before, the parameter δ is obtained experimentally, we have tested δ from 0.01 to 10 and find that 0.2 is good for fusion.

3. Experiments Results

3.1. Quality Indices for Assessing Image Fusion

To demonstrate the effectiveness of our algorithm, we need some objective indices. They are used the to assess the relationship between the fusion images and the original images. In the letter, the following typical metrics are chosen [13, 16, 17]:

1. Correlation Coefficient (CC) [17].

$$CC = \frac{\sum_{i=1}^{M}\sum_{j=1}^{N}[F-\overline{F}][H-\overline{H}]}{\sqrt{\sum_{i=1}^{M}\sum_{j=1}^{N}[F-\overline{F}]^2\sum_{i=1}^{M}\sum_{j=1}^{N}[H-\overline{H}]^2}} \tag{22}$$

where F and H represent the value of the same pixel in two images. $\overline{F}$ and $\overline{H}$ represent the mean value of image F and H, respectively. The index CC evaluates the correlative degree of the fused images and the original images band by band. It has the reference value 1.

2. Spectral Angle Mapper (SAM).

The definition of SAM is

$$\text{SAM} = cos^{-1}(\frac{<\vec{a},\vec{b}>}{\|\vec{a}\|\cdot\|\vec{b}\|}) \tag{23}$$

where $\vec{a},\vec{b}$ represent the same pixel's spectral vectors of the original and fused data, respectively. It is an important index in describing the performance of spectral preservation with the reference value 0. In our experiments, we calculate the SAM with all pixels and use their mean value as our final spectral angle.

3. Universal Image Quality Index(UIQI)

The index is proposed in [18] and defined as:

$$\text{UIQI} = \frac{4\sigma_{HF}\cdot\overline{H}\cdot\overline{F}}{\sigma_H^2+\sigma_F^2\left[(\overline{H})^2+(\overline{F})^2\right]} \tag{24}$$

where $\overline{H}$ and $\overline{F}$ are the mean of original image H and fused image F, respectively. σ_H and σ_F are the variances of H and F, and σ_{HF} is the covariance

between H and F. This index reflects the combination of three different factors: "loss of correlation, luminance distortion, and contrast distortion." It has the reference value 1. In the calculation, since the dependent space of image quality, statistical features of local measure and combination are need. In our experiment, a sliding window with a size of 8×8 is applied.

3.2. Experiment on MSI Fusion

In the first experiment, we obtain the MSI and PI of GeoEye-1 free from the internet `http://www.geoeye.com/CorpSite/`. The MSI has 4 bands (red, green, blue and near-infrared (NI)) with spatial resolution of 2 meters. Before fusion, it is interpolated to 1598×1600 pixels by bicubic interpolation. The PI also has the size of 1598×1600 pixels, and the spatial resolution is 0.5 meters. They are illustrated in Fig. 1. All have value with 11 bits and are registered well before the fusion.

The proposed ISFIM is implemented to make a comparative analysis with other commonly used fusion methods, namely, DWT, GS, and Liu's SFIM. The software environment for visualizing images (ENVI) is used to implement the fusion process with the method GS. In the case of DWT method, three levels of decompositions are used.

To save space, Fig. 2 displays subscenes (the area that in the rectangular frame of Fig. 1(a)) of the original MSI and the fused results by different fusion methods. Normalization is need before showing these data with 11 bits. According to the images in Fig. 2, it is clear that, all the fusion methods have sharpened the MSI effectively, and all subscenes in Fig. 2(b) - (e) are much clearer than that in Fig. 2(a). However, the color in Fig. 2(e) is the closest to that in Fig. 2(a), while the color in Fig. 2(b) - (d) is obviously darkened. This implies that the proposed ISFIM keeps the color information best while obtaining sharpened details.

The indices illustrated in Table I could help us quantitatively evaluate the different fusion methods. The bold font is the best one in the same row. CC-band 1-4 stand for the correlation coefficient between the fused data and the original MSI from band 1 to 4. CC-average is the mean value of the CC-band 1-4. It is clear that, the ISFIM has the best results of all the bands among these fusion methods. It indicates that the fused result obtained by this method is the closest to the source MSI. Also this conclusion could be confirmed by the index UIQI in the bottom row. On the other hand, in the sixth row, both the SFIM and ISFIM have the same value of SAM that close to zero. Actually, from their fusion model, it is easily to arrive at a conclusion

(a)

(b)

Figure 1: Original HSI and PI in experiment 1. (a) The original MSI. (b) The original PI.

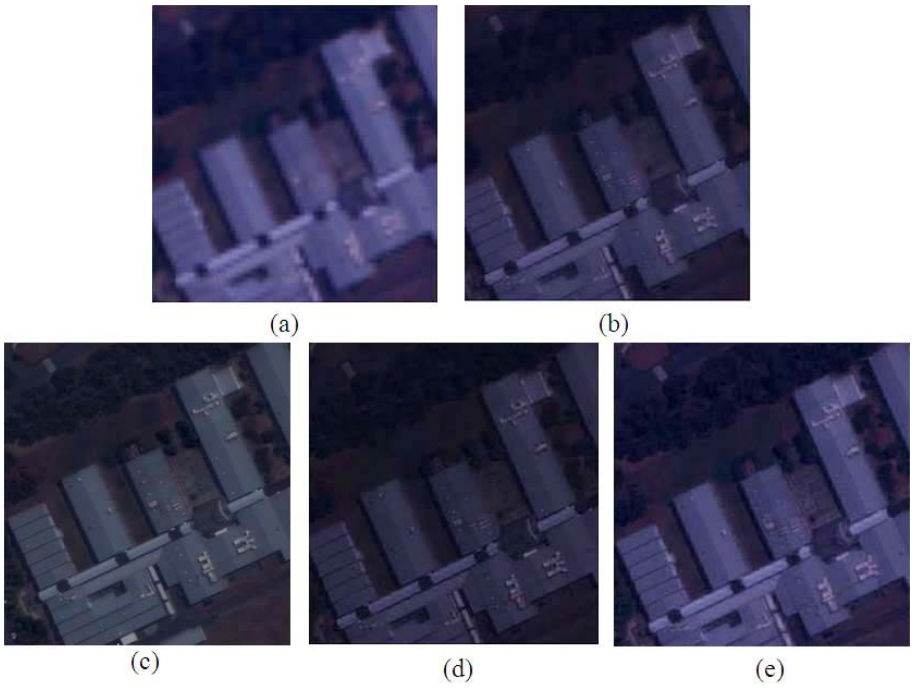

Figure 2: Subscenes of the original MSI and fused MSIs by different methods. (a) The original MSI. (b)-(e) The subscenes of fused MSIs by methods DWT, GS, SFIM, and the proposed ISFIM, respectively.

Table 1: Evaluation results of the simulated experiment

Indices	DWT	GS	SFIM	ISFIM
CC-band 1	0.9322	0.8908	0.8972	**0.9319**
CC-band 2	0.9166	0.8776	0.9196	**0.9483**
CC-band 3	0.9337	0.8851	0.9370	**0.9605**
CC-band 4	0.8819	0.9505	0.9284	**0.9518**
CC-average	0.9161	0.9010	0.9206	**0.9482**
SAM	6.9746	1.9849	**0.00017**	**0.00017**
UIQI	0.5558	0.4971	0.5355	**0.5578**

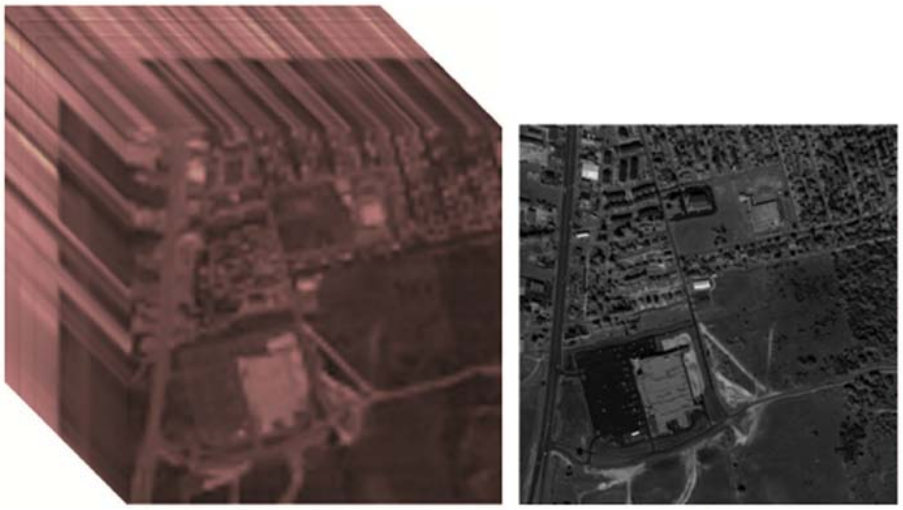

Figure 3: Original HSI and PI in experiment 2. (a) The original HSI. (b) The original PI.

that, the value of SFIM and ISFIM are precisely equal to zero because the spectral line is multiplied by a same parameter in each band. However, the performance of ISFIM is better in MSI fusion synthetically in visual analysis and quantitatively evaluation.

3.3. Experiment on HSI Fusion

The ISFIM does not limit the number of bands and is also available in HSI fusion. We use the HSI free from `https://engineering.purdue.edu/~biehl/MultiSpec/hyperspectral.html`. It has the size of 307 $\times$ 307 pixels. In order to simulate the original images, we first pick the bands of the original data with the $0.5-0.76\ \mu m$ region, and treat the mean of them as the original PI for fusion. After removing some bands, 100 bands are preserved as HSI. Then, we spatially degrade each band of the HSI with decimation by four. Finally, the degraded HSI is upsampled to 307 $\times$ 307 pixels by bicubic interpolation, and we obtain the source HSI data for fusion. Thus, the original two different source images are registered by default and shown in Fig. 3.

In experiment 2, methods DWT, GS, SFIM and ISFIM are also implemented, and the fused results are presented in Fig. 4. The quantitative

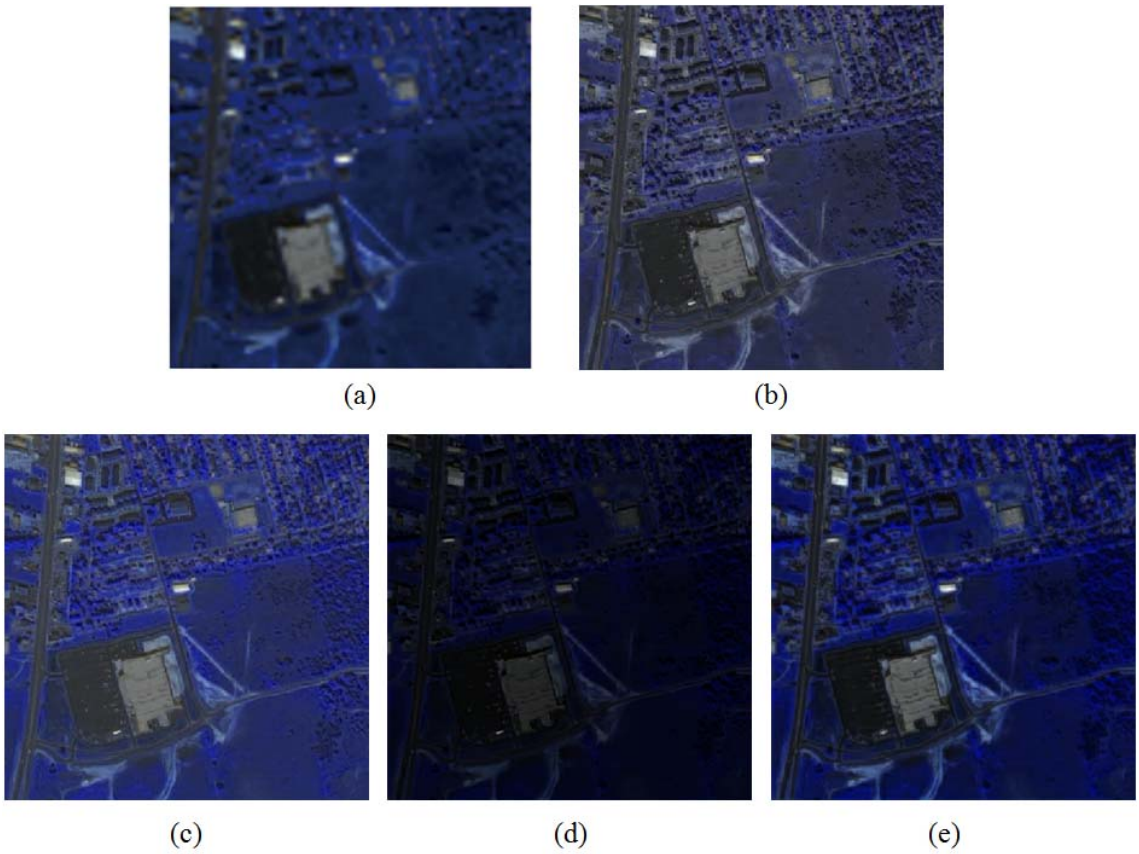

Figure 4: Original HSI and fused images in experiment 2. (a) The original HSI. (b)-(e) are the fused results with the other methods DWT, GS, SFIM and the proposed ISFIM method. All the images are shown in false color with bands 10, 30, 60.

Table 2: Evaluation results of the simulated experiment

Indices	DWT	GS	SFIM	ISFIM
CC-average	0.8532	0.8882	0.8382	**0.9173**
SAM	3.7138	11.0082	**0.00017**	**0.00017**
UIQI	0.5269	0.5097	0.4746	**0.5793**

evaluation results are presented in Table II. Since there are too many bands in HSI, only CC-average is displayed. Also, the bold font is the best one in the same row.

By visually comparing the fused images with the original source image, it is clear that the HSIs are sharpened effectively contrast to the original HSI in Fig. 4(a). However, DWT and GS fade the green color of the original HSI in Fig 4(b) and (c). On the other hand, SFIM darkens the green color in Fig. 4(d) (It also happens in MSI fusion). ISFIM keeps the color of Fig. 4(a) while sharpening the details effectively. In Table II, we see that, the ISFIM also has the best value in CC, SAM, UIQI, which indicates that, the proposed ISFIM also behaves well in HSI fusion.

4. Conclusion

In the letter, an ISFIM fusion method is proposed. A new kind of relationship between the DN value of fused data and the original data is obtained. The fusion model partly revises the original SFIM by introducing the process of calibration, which is one of the crucial step in the remote sensing. From the discussion, we see that, SFIM is a special form of ISFIM while the value of offset in the calibration process is zero. On the other hand, we see that, it is not always possible to obtain the precise parameters of gain and offset in the calibration process. Therefore, we relax the ISFIM by using experiential constants. At last, in the experiments on MSI and HSI data, visual analysis and quantitative evaluations assess the performance of different fusion methods. It is clear that, the fused data obtained by the ISFIM preserves the color of the original MSI/HSI best while effectively sharpening the details. Better quantitative indices, like SAM, UIQI and CC, are obtained by the method ISFIM. It imply that, the ISFIM a good improvement for SFIM.

References

[1] P. S. Chavez and J. A. Bowell, Comparison of the spectral information content of Landsat thematic mapper and SPOT for three different sites in the Phoenix, Arizona region. Photogramm. Eng. Remote Sens. 54(12) (1998) 1699-1708.

[2] T. M. Tu, S. C. Su, H. C. Shyu, and P. S. Huang, A new look at IHS-like image fusion methods, Inf. Fusion 2(3) (2001) 177-186.

[3] C. A. Laben and B. V. Brower, Process for enhancing the spatial resolution of multispectral imagery using pan-sharpening U. S. Patent 6011875, Jan. 4, (2000).

[4] M. J. Shensa, The discrete wavelet transform: Wedding the a Trous and Mallat algorithms, IEEE Trans. Signal Process. 40(10) (1992) 2464-2482.

[5] J. Nunez, X. Otazu, O. Fors, A. Prades, V. Pal, and R. Arbiol, Multiresolution-based image fusion with additive wavelet decomposition, IEEE Trans. Geosci. Remote Sens. 37(3) (1999) 1204-1211.

[6] T. Ranchin, B. Aiazzi, L. Alparone, S. Baronti, and L. Wald, Image fusionThe ARSIS concept and some successful implementation schemes, ISPRS J. Photogramm. Remote Sens. 58 (2003) 4-18.

[7] P. Blanc, T. Blu, T. Ranchin, L. Wald, and R. Aloisi, Using iterated rational filter banks within the ARSIS concept for producing 10 m Landsat multi-spectral images, Int. J. Remote Sens. 19(12) (1998) 2331-2343.

[8] M. L. S. Aguena and N. Mascarenhas, Multispectral image data fusion using projections onto convex sets techniques, in Proc. XV Braz. Symp. Comput. Graph. Image Process. (2002) 76-82.

[9] Zhenwei Shi, Zhenyu An, and Zhiguo Jiang, Hyperspectral image fusion by the similarity measure based variational method, Opt. Eng. 50(7) (2011) 077006.

[10] M. Ehlers, Spectral characteristics preserving image fusion based on Fourier domain filtering, Proc. SPIE-Remote Sens. Environ. Monit., GIS Appl., Geol. IV, Maspalomas, Gran Canaria, Spain, (2004).

[11] J. G. Liu, Smoothing Filter-based Intensity Modulation: a spectral preserve image fusion technique for improving spatial details, I. J. Remote Sensing 21(18) (2000) 3461-3472.

[12] M. Dinguirard, P. N. Slater, Calibration of Space-Multispectral Imaging Sensors: A Review, Remote Sensing of Environment 68(3) (1999) 194-205.

[13] Y. Chen, Z. Xue, and R. S. Blum, Theoretical analysis of an information-based quality measure for image fusion, Inf. Fusion, 9(2) (2008) 161-175.

[14] J. G. Liu, Reply. Int. J. Remote Sens. 23(3) (2002) 598-601.

[15] L. Wald, T. Ranchin, Comment: Liu "Smoothing filter-based intensity modulation: A spectral preserve image fusion technique for improving spatial details", Int. J. Remote Sens. 23(3) (2002) 593-597.

[16] M. Deshmukh, U. Bhosale, Image fusion and image quality assessment of fused images, International Journal of Image Processing 4(5) (2010) 484-508.

[17] V. Vijayaraj, C. G. O. Hara, N. H. Younan, Quality analysis of pan-sharpened images, IEEE International Geoscience and Remote Sensing Symposium 1 (2004) 20-24.

[18] Z. Wang, A. C. Bovik, A universal image quality index, IEEE signal processing letters 9(3) (2002) 81-84.